TWENTYFITH EUROPEAN ROTORCRAFT FOROM

Paper n°B5

NOISE SOURCE LOCALIZATION ON A DAUPHIN HELICOPTER IN FLIGHT

BY

D. BLACODON*, G. ÉLIAS*, D. PAPILLIER+ and J. PRIEUR*

* Office National d'études et de Recherches Aérospatiales (ONERA), 92322 Châtillon, France
+ Centre d'Essais en Vol (CEV) – Base d'Essais d'Istres 13128 Istres Air, France.

SEPTEMBER 14-16, 1999
ROME
ITALY

ASSOCIAZIONE INDUSTRIE PER L'AERSPAZIO, I SISTEMI E LA DIFESA
ASSOCIAZIONE ITLIANA DI AERONAUTICA ED ASTRONAUTICA

NOISE SOURCE LOCALIZATION ON A DAUPHIN HELICOPTER IN FLIGHT

D. BLACODON*, G. ÉLIAS*, D. PAPILLIER+ and J. PRIEUR*

* Office National d'études et de Recherches Aérospatiales (ONERA), 92322 Châtillon, France
+ Centre d'Essais en Vol (CEV) – Base d'Essais d'Istres 13128 Istres Air, France.

Abstract
A flight test campaign has been performed on a Dauphin helicopter with the participation of Istres Flight Test Center (CEV). The objective was to study the feasibility of helicopter noise source localization using microphone antenna methods developed at ONERA and already implemented for aircraft noise studies. The method proves successful, clearly identifying noise sources from the main rotor or the fenestron depending on the frequency band and the flight conditions.

I. Introduction

Among the fields in helicopter research, the improvement of the knowledge of noise generating mechanisms is of a great interest for helicopter industry. It is particularly important to reduce the acoustic pollution radiated by this vehicle for using it as a means of transportation in urban areas. Many tests have been performed in wind tunnels to better understand such an important phenomenon as BVI (Blade-Vortex Interaction) which dominates helicopter noise radiation in descent flight. Numerous papers deal with the prediction of this particular type of noise [1, 2, 3]. In the present paper, another way is explored to identify the origin of the major noise sources of a helicopter. It consists in performing their location during flight tests at typical flight conditions like hover, descent or level flight.

Acoustic flight tests on a helicopter have been performed with the participation of the Istres Flight Test Center (CEV). The objective was to study the feasibility of helicopter noise source localization using the acoustic imaging developed at ONERA and already implemented during wind tunnel tests on model aircraft [4], helicopter rotors [5] and aircraft flight tests.

Two methods are considered in this study. The first one (Method 1 [6]) is based on the data collected by a cross-shaped array at rest on the ground. It provides the acoustic source locations in the frequency band of interest [0, 3 kHz] and answers some questions asked the industrials. The technique allows identifying the acoustic radiating areas on the helicopter in frequency domain. This knowledge is very helpful in determining the elements of the helicopter which significantly contribute to the far field noise.

The second one (Method 2 [5]) uses microphones mounted on the helicopter fuselage to locate the BVI noise sources radiating in descent flights. This method, which works in the time domain, allows isolating and locating any very impulsive peak (as a BVI event) in the acoustic signature.

Dealing with moving sources, a method is needed in order to correct the cross-shaped array microphone signals from the Doppler effect and locate the sources in the helicopter reference frame. An optical trajectography system was developed by CEV to locate during the flights and at each time the helicopter position and its orientation relative to the ground array. The trajectography data, the cross-shaped array and the on-board microphones signals have to be synchronized. This is achieved using the clock of a GPS and a EDITH device.
This paper begins with a brief review of the two localization methods (Secs. II and III). The experimental configuration and the data acquisition are described in Sec. IV. Method 1 and Method 2 are applied to tests performed with the Dauphin helicopter in Sec. V.

II. Method 1 – Localization of moving source noise from an array of transducers at rest

A. The sound pressure field on an array of transducers due to a moving source

Consider the configuration sketched in Fig. 1. A helicopter with a coordinate system $R_H(o_H, \vec{x}_H, \vec{y}_H, \vec{z}_H)$ is moving with respect to a ground referential $R_G(o_G, \vec{x}_G, \vec{y}_G, \vec{z}_G)$ along a trajectory near an antenna of N microphones at rest. The sound pressure $s(t)$ emited at time t by a moving source S of the helicopter is measured by the microphone M_n at time:

$$t_R = t + \tau_n^S(t), \tag{1}$$

where $\tau_n^S(t) = \frac{R_n^S(t)}{c}$ is the time delay between S and M_n. $R_n^S(t)$ denotes the distance between S and M_n at the emission time t and c is the speed of sound.

The relation below provides the acoustic pressure field at microphone M_n with respect to the source location at time t:

$$p_n(t+\tau_n^S(t)) = \frac{s(t)}{c\tau_n^S(t)}. \quad (2)$$

We assume that the sources are in the Fresnel region of the transducer array. In this case, the incident wave-field on the array can be expressed as a sum of monopoles. For simplicity, we shall consider a source defined by a single monopole at frequency f_s

$$s(t) = Ae^{2\pi i f_s t} \quad (3)$$

B. Principles of localization method

We wish to determine the location and the amplitude of S from the measurements $p_n(t)$ $(n = 1,2,...,N)$. The first step in solving this problem consists in searching the amplitude and the location of a monopole, at every point F of a domain assumed to contain S (Fig. 1). The solution cannot be exact since the signals are generally corrupted by background noise and the propagation medium can be slightly inhomogeneous. Nevertheless, the error involved in the approximate solution can be minimized by the least square error for a measurement over a time T:

$$E(s,F) = \int_T \sum_{n=1}^{N} \left(p_n(t+\tau_n^F(t)) - \frac{s(t)}{c\tau_n^F(t)} \right)^2 dt \quad (4)$$

For a focus point F, a minimization with respect to $s(t)$ leads to [7]:

$$s^F(t) = \frac{\sum_{n=1}^{N} \frac{p_n(t+\tau_n^F(t))}{c\tau_n^F(t)}}{\sum_{n=1}^{N} \frac{1}{(c\tau_n^F(t))^2}} \quad (5)$$

In the assumption that the sound pressure is radiated by a single monopole, it is easy to show that $s^F(t) = s(t)$ for $F \equiv S$.

Furthermore, the spectral density $S^F(f)$ of $s^F(t)$ is then an estimator of $S(f)$ the one of $s(t)$. In the case of the monopole (3), we have $S^S(f) = S^F(f)$.

C. Cross-Shaped array processing

We now turn our attention to two-dimensional noise sources localization which is the majority of situations encountered in practice. The conventional processing requires measuring the acoustic pressure radiated by a planar array including many microphones. It is shown in [6] that a result nearly similar can be obtained using a cross-shaped array in addition with an appropriate processing. This solution is obviously cheaper since the number of transducers needed is much less important. Working in the frequency domain, this latter processing is based on this estimator:

$$I(F,f) = < R_e[S_A^{*F}(f) S_B^F(f)] > \quad (6)$$

where $S_A^F(f)$ is the Fourier transform of the signal $s_A^F(t)$ (5) estimated from the measurements performed by the microphones of the arm A of the array. $S_B^F(f)$ is obtained from the arm B, * denotes the complex conjugated and $< >$ is the statistical average.

The maximum of $I(F,f)$ is obtained in a case of a single monopole for $F \equiv S$. The results presented in Sec. IV.B are given by (6).

D. General considerations

The implementation of Method 1 involves the knowledge at every time t of:

a) the trajectory $R_n^F(t)$ to compute the time delay $\tau_n^F(t)$,

b) a time reference to synchronize $p_n(t)$ and $\tau_n^F(t)$, in order to dedopplerize each measurement signal $p_n(t)$ by computing $p_n(t+\tau_n^F(t))$.

In the next section, we will discuss in some details of the computation of $R_n^F(t)$ and how the synchronization processing is implemented.

Computation of the trajectory of a focus point

The time delay $\tau_n^F(t)$ depends on the distance $R_n^F(t)$ between a focus point F and the microphone M_n:

$$R_n^F(t) = \left| \overrightarrow{o_G F(t)} - \overrightarrow{o_G M_n} \right| \tag{7}$$

where

$$\begin{aligned} \overrightarrow{o_G F(t)} &= x_F(t)\vec{x}_G + y_F(t)\vec{y}_G + z_F(t)\vec{z}_G \\ \overrightarrow{o_G M_n} &= x_n\vec{x}_G + y_n\vec{y}_G + z_n\vec{z}_G \end{aligned} \tag{8}$$

Nevertheless, the vector $\overrightarrow{o_G F(t)}$ cannot be measured for every focus point during the flight tests. In our application, only the components of the camera C_{am} mounted under the nose of the helicopter are known in R_G. There are defined by:

$$\overrightarrow{o_G C_{am}(t)} = x_{cam}(t)\vec{x}_G + y_{cam}(t)\vec{y}_G + z_{cam}(t)\vec{z}_G \tag{9}$$

Obviously, $\overrightarrow{o_G F(t)}$ can be expressed using $\overrightarrow{o_G C_{am}(t)}$ in conjunction with the attitude parameters of the helicopter collected during the tests by the inertial platform unit. This device gives the angles $\theta(t)$, $\phi(t)$ and $\psi(t)$ in the earth reference $R_E(o_E, \vec{x}_E, \vec{y}_E, \vec{z}_E)$ (Fig. 2). $\theta(t)$, $\phi(t)$ and $\psi(t)$ describe respectively pitch, roll and yaw of the helicopter. Furthermore, an angle ζ exists between R_E and R_G which is also considered to build $\overrightarrow{o_G F(t)}$.

Lets us now introduce the components of F and C_{am} in R_H:

$$\begin{aligned} \overrightarrow{o_H F} &= \mathrm{X}_F\vec{x}_H + Y_F\vec{y}_H + Z_F\vec{z}_H \\ \overrightarrow{o_H C_{am}} &= \mathrm{X}_{Cam}\vec{x}_H + Y_{Cam}\vec{y}_H + Z_{Cam}\vec{z}_H \end{aligned} \tag{10}$$

Now, we may write $\overrightarrow{o_G F(t)}$ in the following form using Eqs. (8) and (10):

$$\overrightarrow{o_G F(t)} = \overrightarrow{o_G C_{am}(t)} + \overrightarrow{C_{am} F} \tag{11}$$

A transition from helicopter coordinate system R_H to ground coordinate system R_G is required to express $\overrightarrow{C_{am} F}$ in R_G, since the components of $\overrightarrow{o_G C_{am}(t)}$ are known in R_G and those of $\overrightarrow{C_{am} F}$ in R_H. This transformation needs to cascade four rotations, $R_\phi R_\theta R_\psi R_\zeta$ [8] from which $\overrightarrow{C_{am} F}$ can be written as:

$$\overrightarrow{C_{am}F} = \left[X_F - X_{cam};\quad Y_F - Y_{cam}\quad Z_F - Z_{cam}\right] R_\varphi R_\theta R_\psi R_\zeta \begin{bmatrix} \overrightarrow{x_G} \\ \overrightarrow{y_G} \\ \overrightarrow{z_G} \end{bmatrix} \tag{12}$$

Three successive rotations R_φ, R_θ and R_ψ are used to express $\overrightarrow{C_{am}F}$ from R_H to R_I and the fourth one R_ζ is needed to write the previous result in R_G. This procedure is implemented to estimate $\overrightarrow{o_G F(t)}$ from which it is possible to construct the trajectory $R_r^F(t)$ for every focus points F.

Time reference

The source localization technique is based on the cancellation of the Doppler effect in the N measurement signals $p_n(t)$. For a focus point F, the dedopplerisation operation is based on the computation of the time delay $\tau_n^F(t)$ to produce the signal $p_n(t+\tau_n^F(t))$ from $p_n(t)$ [7]. $p_n(t)$ and $\tau_n^F(t)$ are obtained separately, since $p_n(t)$ comes from the microphones at rest in R_G, and the $\tau_n^F(t)$ is estimated from $\overrightarrow{o_G C_{am}(t)}$, $\theta(t)$, $\phi(t)$ and $\psi(t)$ recorded for the moving helicopter in R_G. Thus, it is necessary to have a time reference to synchronize ground and on board data to compute $p_n(t+\tau_n^F(t))$. To achieve this, the time provided by a GPS (Global Positioning System) device has been recorded simultaneously with the acoustic measurements, while the time supplied by a EDITH clock has been recorded with the on board parameters. The synchronization operation consists first in reading GPS and EDITH recorded time. One can then establish a connection between the data $p_n(t)$ and $\tau_n^F(t)$ which have the same date t.

III. Method 2 – Localization of an impulsive source noise at rest from moving transducers

In the previous section, the localization processing by Method 1 is performed in frequency domain with signals $p_n(t)$ due to the whole radiated noise. Another approach is to take advantage of the impulsive nature of BVI noise to isolate each peak on the acoustic time signature, before to carry out the localization in time domain. However, this solution is applicable only if the peaks relating to BVI noise are weakly altered either by acoustic propagation or by other noise sources. To reduce the possible effect of degradations, the data for Method 2 are measured by microphones mounted on the helicopter at locations where the BVI noise is intense.

A. Source model

The BVI noise can be conveniently modeled by a rotating point source S at times $t_m = t_E + mT$ by:

$$s(t) = A\delta(t - t_m) \tag{13}$$

where t_E is one of the emission time, T is the rotation period of S, m is an integer and $\delta = 1$ for $t = t_m$ and 0 for different t.

During a single rotation, the sound pressure radiated by S in a referential at rest $R_1(o_1, \vec{x}_1, \vec{y}_1, \vec{z}_1)$ is measured by a moving microphone M_n with respect to R_1 (Fig. 3), under the following form:

$$p_n(t) = s(t - t_n^R) \tag{14}$$

where $t_n^R = t_E + \tau_n^S(t)$ is the reception time, which is assumed to be known on the acoustic signatures of each microphone (see Fig. 4).

B. Source localization by Method 2

Again, we want to estimate the location of S and its amplitude. Since the nature of the BVI noise is impulsive, this problem can be conveniently solved in time domain by a method based on a multiplicative processing [5]:

$$H(t,F) = \left[\prod_{n=1}^{N} R_n^F(t) P_n(t+\tau_n^F(t))\right]^{\frac{1}{N}} \tag{15}$$

where F is a focus point belonging to an area enclosing the rotor disk at time t_E.

From the definition of $s(t)$ (13) and of $p_n(t)$ (14) Eq. (15) becomes :

$$H(t,F) = A\left[\prod_{n=1}^{N} \frac{R_n^F(t)A\delta(t-t_E+\tau_n^F(t)-\tau_n^S(t))}{R_n^S(t)}\right]^{\frac{1}{N}} \tag{16}$$

It is possible to show from Eq. (16) that the amplitude A of the source noise is retrieved when the computation is carried out at the emission time $t = t_E$ and for $F \equiv S$.

As for Method 1, the time delay

$$\tau_n^F(t) = \frac{\left|\overrightarrow{o_1F} - \overrightarrow{o_1M_n(t)}\right|}{c} \tag{17}$$

must be known at every time t to achieve the BVI localization. To do this, a transition from coordinate systems R_H to R_1 is required, since the noise sources are at rest in R_1 and the microphones are moving in this referential system. To go further, we assume that during an analyzing time T, the microphones moves along a straight line parallel to the $\overrightarrow{x_1}$ direction, with constant speed V. Then the equation for $\tau_n^F(t)$ reduces to:

$$\tau_n^F(t) = \frac{\sqrt{\left(X_F - V(t_n^R - t)\right)^2 + \left(Y_F - y_n\right)^2 + \left(Z_F - z_n\right)^2}}{c} \tag{18}$$

To summarize this section, the main steps in the localization processing of BVI noise are described. First, the BVI peaks are isolated in each acoustic signature. Then, the localization processing consists in computing $H(t,F)$ at a given time t for all focus points F, scanning the space where a source may exist. This gives an elementary map which is nonzero only if $t = t_E$ and $F \equiv S$. Calculation is repeated for all values of t belonging to a time interval T. Finally, the location of BVI noise is obtained by summing all the elementary maps with nonzero amplitude.

IV. Experimental configuration and data acquisition

The methods presented in this paper are applied to a flight campaign on a research Dauphin (Fig. 5) performed in December 1998 in Istres Flight Test Center (CEV).

Ground Reference

A dashed line has been painted on the main road of CEV to guide the pilot during the tests. It also corresponds to the y_G axis of R_G, while the x_G axis is the arm A of the cross-shaped antenna and z_G axis is oriented toward the sky.

Ground antenna of microphones

The noise radiated in the farfield by the Dauphin during flyover was collected by a cross shaped array (Fig. 5) with twenty nine microphones AKSUD ½-inch periodically space every fifty centimeters on the two arms of the array of seven meters long each. The locations of microphones needed by Method 1 have been measured with a very good accuracy by a CEV team with a theodolite in the R_G coordinate system.

On board microphones

The acoustic measurements on-board the helicopter were made with twenty microphones mounted outside the Dauphin (Fig. 6): four on the roof, two on each door; eight on the left empennage and four on the right one. All the microphones Brüel & Kjaer model 4135, ½-inch were equipped with nose cone to reduce the aerodynamic noise produced during the flight-tests. The microphone locations needed by Method 2 where also measured with the aid of a theodolite in the R_H coordinate system.

Vehicule tracking

The vehicle tracking device has been developed by CEV to provide the components of a camera IS 802 mounted under the nose of the Dauphin in the ground referential. The video images recorded during the flights by the camera allow to estimate the horizontal locations $x_{cam}(t)$, $y_{cam}(t)$. A radio probe provides the vertical location $z_{cam}(t)$. The major

drawback of this trajectory system is due to the poor angular aperture of the trajectory camera, which reduces the tracking processing in an angular sector of ±50°. Furthermore, since $x_{cam}(t)$, $y_{cam}(t)$, $z_{cam}(t)$, $\theta(t)$, $\phi(t)$ and $\psi(t)$ are known sixty-four times per second, an interpolation from $64Hz$ to $25kHz$ sampling rate is performed on these data for the synchronization operation with the signals $p_n(t)$ sampled at $25kHz$.

V. Flight test results

The first results presented concern the source localization by Method 1. Then the localization of blade vortex interaction by Method 2 is examined.

A. Source localization by Method 1

Method 1 is illustrated by different cases corresponding to a hover, a flyover and a descent-flight in this Section.

Test 1 – Hover. $H = 52$ m

In this first test the helicopter performs a hover above the cross-shaped antenna at a height of $H = 52$ m. The objective of this experiment is to validate the localization technique in a simple case where there is no Doppler effect on the signals of the microphone array and where the aerodynamic perturbation is negligible.

A frequency spectrum measured by microphone 8 at the center of the antenna is shown in Fig. 7a. The two main features are 1) the very broadband combustion noise around $300Hz$; and 2) several tones at $2kHz$ and $3kHz$ due to the second and the third harmonic of the fenestron. Results obtained at $2kHz$ and $3kHz$ are shown respectively in Figs. 7b and 7c. As expected the main noise source is found near the fenestron. A more accurate localization is observed at $2kHz$ than at $3kHz$. Despite this slight difference, both results confirm the validity of Method 1.

Test 2 –Flyover. $V = 113\,kts$. $H = 15$ m

The aims of this flight are:

firstly, to check the dedopplerisation procedure discussed in Sec II. D.;

secondly, to demonstrate the capability of Method 1 to localize narrow band noise sources.

In order to satisfy these objectives, we consider the localization of the fenestron noise which is not quite pure tones. The fenestron noise produces two peaks at $2kHz$ and $3kHz$ with a bandwidth of $300Hz$ (Fig. 8a) as one can see in Fig. 9a. The localization is carried out at three successive frequencies (with a bandwidth $\Delta f = 49Hz$), from $1855Hz$ to $1953Hz$. As expected, the main noise sources are located near the fenestron (Figs 8b, 8c and 8d).

Test. 3 – Method I and Descent flight- $V = 61\,kts$ – $\beta = 8{,}3°$

Since the trajectory parameters needed for the dedopplerization operation are only available for $-50° \le \eta \le 50°$ (see Sec. II. D.), the localization is performed for an observation angle $\eta = 50°$. The acoustic signature (Fig. 9a) and the spectrum (Fig. 9b) of microphone 8 show that the BVI noise is mixed with a very high broadband noise.

The localization is carried out at frequencies $f_1 = 781Hz$, $f_2 = 1661Hz$, $f_3 = 2490Hz$ and $f_4 = 3466Hz$, in a space region limited to the rotor disk where the BVI phenomenon occurs. The noise sources referenced by letters A to D are found on the advancing side of the disk in the first quadrant in azimutal range between 0° and 40° (Figs. 9c to 9.e and Table 1). This result is in agreement with previous numerical and wind tunnel studies [1] for f_3 and f_4 but not for f_1 and f_2. This is not too surprising since measurement signals characterize not only BVI noise but whole noise radiated by the helicopter. At frequencies f_1 and f_2 the BVI noise must not be dominant, and this is why the locations found by Method 1 do not correspond to those expected.

Source	Frequency (Hz)	Azimuth φ (°)
A	$f_1 = 781Hz$	0
B	$f_2 = 1661Hz$	20
C	$f_3 = 2490Hz$	40
D	$f_4 = 3466Hz$	40

Table. 1 . Azimuth of BVI locations versus frequency for Test. 3.

B. Source localization by Method 2

Method 2 is applied to the test already analyzed by Method 1, in order to compare the BVI localization by both methods.

The localization processing is carried out with the signals of microphones 13, 14, 16, 16, and 18 which are very receptive to BVI noise.

Test. 4 – Method 2 and Descent flight- $V = 61\,kts - \beta = 8{,}3°$

The flight parameters are the same as those used in Test 3. Fig.11a shows the acoustic signatures on Microphones 13, 14, 15, 16, and 18 measured on one rotation period. The peaks caused by the first and the third blade are higher than those produced by the others blades.

The BVI noise associated with peak A (Fig. 10a) is localized on the advancing side of the disk in the first quadrant in the azimutal range between 45° and 75° (Fig. 10b). This result is similar to that obtained by Method 1 at frequencies $f_3 = 2490Hz$ and $f_4 = 3466Hz$ (Figs. 9e and 9f).

VI. Conclusion

Localization of noise sources radiated by a helicopter in flight is examined by two methods. The first one works in the frequency domain from acoustic measurements by a cross-shaped array of microphones at rest. An optic trajectory and a time reference are used to accomplish the dedoplerisation operation needed in localization processing at each frequency of interest.

The second technique works in time domain to determine BVI noise location from microphones mounted on the helicopter.

Both methods have been applied to tests performed in CEV Istres in December 1997 on a Dauphin helicopter. The results presented in this paper have proven their efficiency to study the noise radiated by a helicopter during flight tests.

ACKNOWLEDGMENT

We wish to express our grateful thanks to J. Chombart, B. Mazin, D. Zuba, P. Lebigot and F. Desmerger for their participation in the experiment and to M. J Bonnet, J. F. Piet, P. Spiegel and to P. Malbéqui for many heplful discussions.

References

1. P. Beaumier, -P. Spiegel - Validation of ONERA Aeroacoustic Prediction Methods for Blade-Vortex Interaction using HART Tests Results. 51st Annual Forum and technology Display of the AHS, Fort Worth, TX, (USA), May 1995.

2. M. C. Joshi -S.R. Liu ,-D.A. Boxwell - Prediction of the blade-vortex interaction noise. 43rd Annual Forum of the American Helicopter Society, Saint-Louis (USA), 1987.

3. K. J. Schultz ,-W.R. Splettstoesser - Prediction of helicopter rotor impulsive noise using blade pressures. 43rd Annual Forum of the American Helicopter Society, Saint-Louis (USA), 1987.

4. J. F. Piet. -G. Élias - Airframe noise source localization using a microphone array. AIAA paper 97-1643, Atlanta (USA), May 1997.

5. D. Blacodon -M. Caplot, -G. Elias - A source localisation technique for helicopter rotor noise. AIAA Paper 87-2743, 11 th Aeroacoustics Conference, Palo Alto (USA). October 1987.

6. G. Élias - Localization with a two dimensional focused array : Optimal signal processing for a cross-shaped array. Inter-Noise 1995, Newport Beach (USA). July 1995.

7. J. F. Piet -G. Elias -P. Lebigot - Localization of acoustic source from a landing aircraft with a microphone array, AIAA Paper 99-1811, 5th AIAA/CEAS Aeroacoustics Conference, Seattle, USA, May 1999.

8. H. Goldstein - Classical mechanics. Addison-Wesley, Reading, MA, 1980.

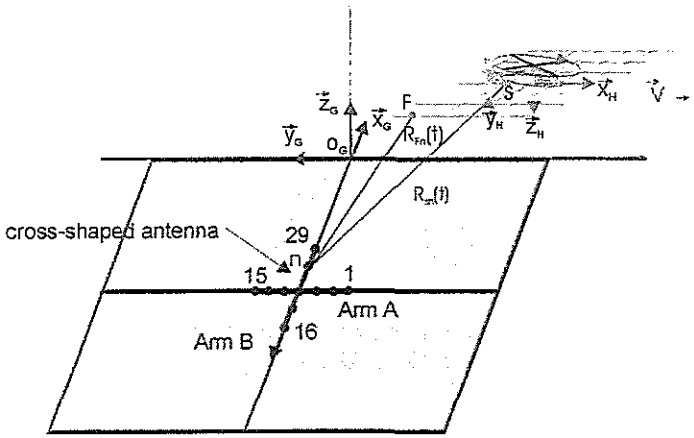

FIG. 1. Geometry of the localization problem of moving noise sources from acoustic measurements at rest.

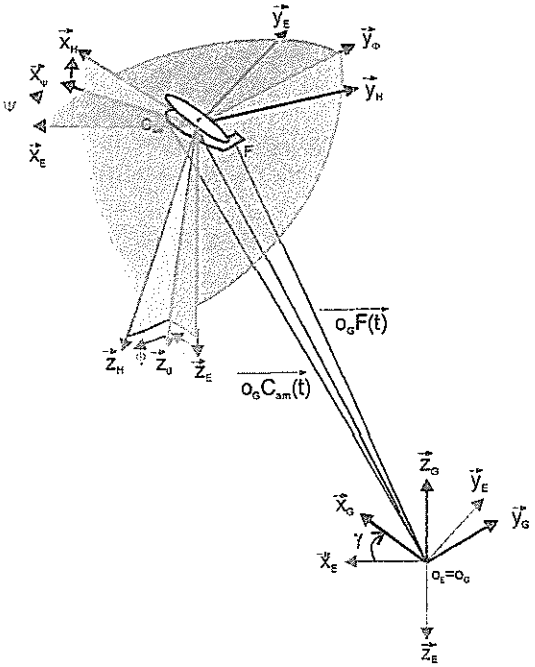

FIG. 2. Coordinate systems used for the dedoplerisation processing of acoustic measurements by the microphones in Fig.1.

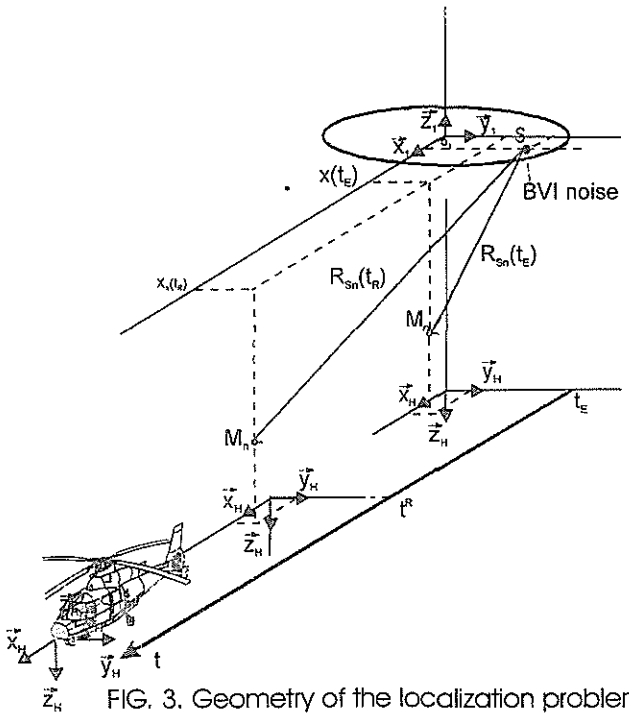

FIG. 3. Geometry of the localization problem of noise sources (BVI) at rest from moving acoustic measurements by microphones located on the helicopter.

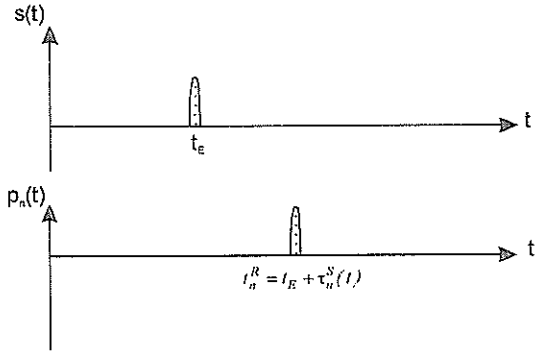

FIG. 4. Example of BVI peak emited by a source S and measured by the n[th] microphone mounted on the helicopter.

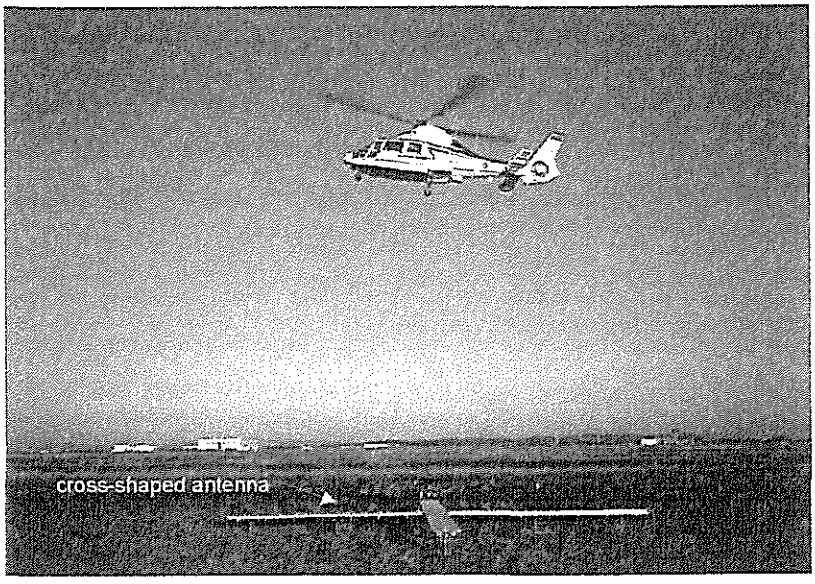

FIG. 5. The Dauphin helicopter during a flight test.

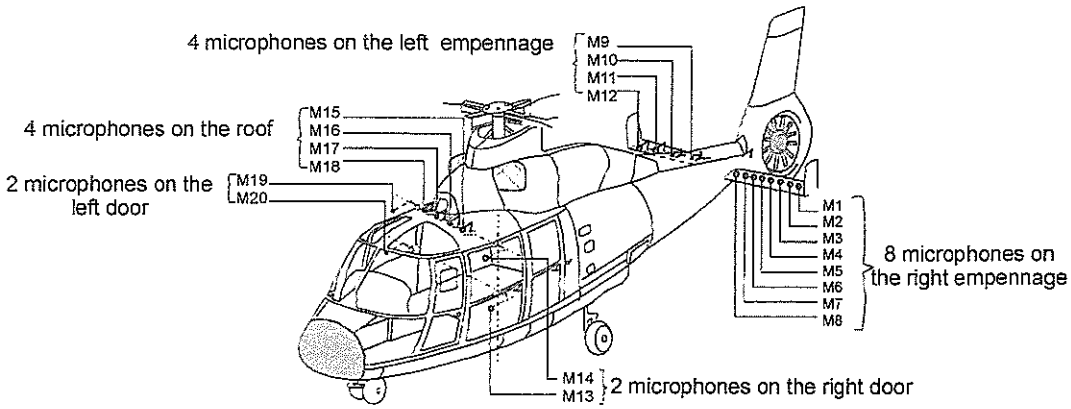

FIG. 6. Location of the 20 microphones mounted on the Dauphin helicopter during the acoustic flight tests.

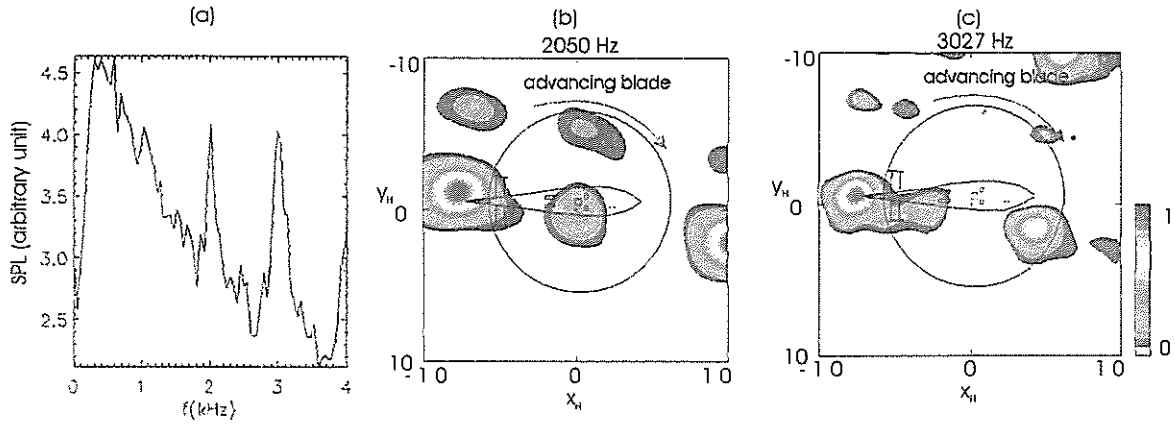

Fig. 7. Hover - V =0 - H=52.
(a) Spectrum of acoustic signature of Microphone 8 of the array.
Localization processing by Method 1 at : (b) 2050 Hz; (c) 3027 Hz.

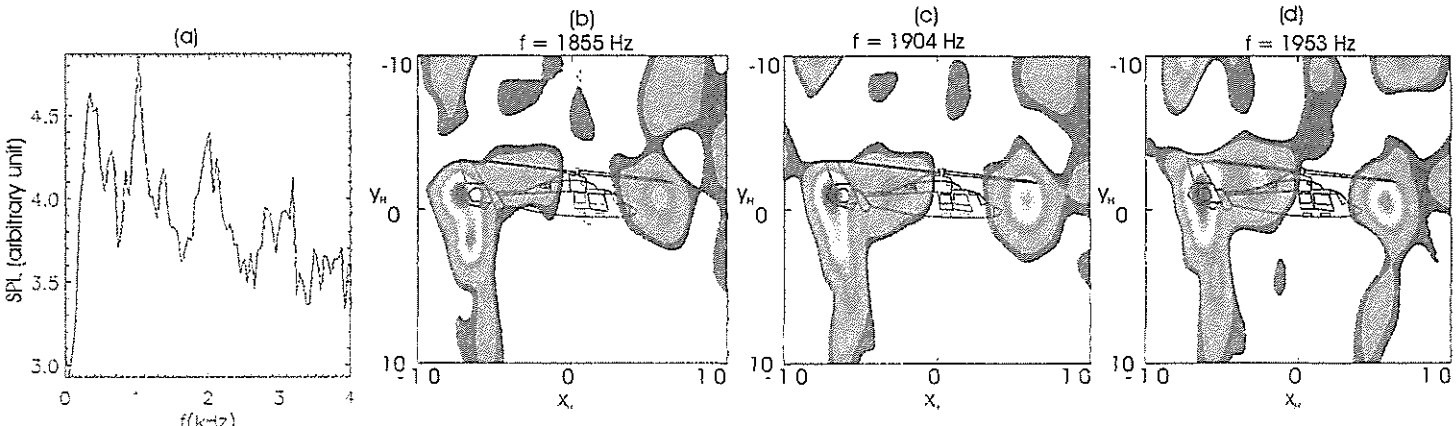

Fig. 8. Fly over - V = 113kts - H=15 m.
(a) Spectrum of acoustic signature of Microphone 8 of the array.
Localization processing by Method 1 at : (b) 1855 Hz; (c) 1904 Hz;
(d) 1953 Hz.

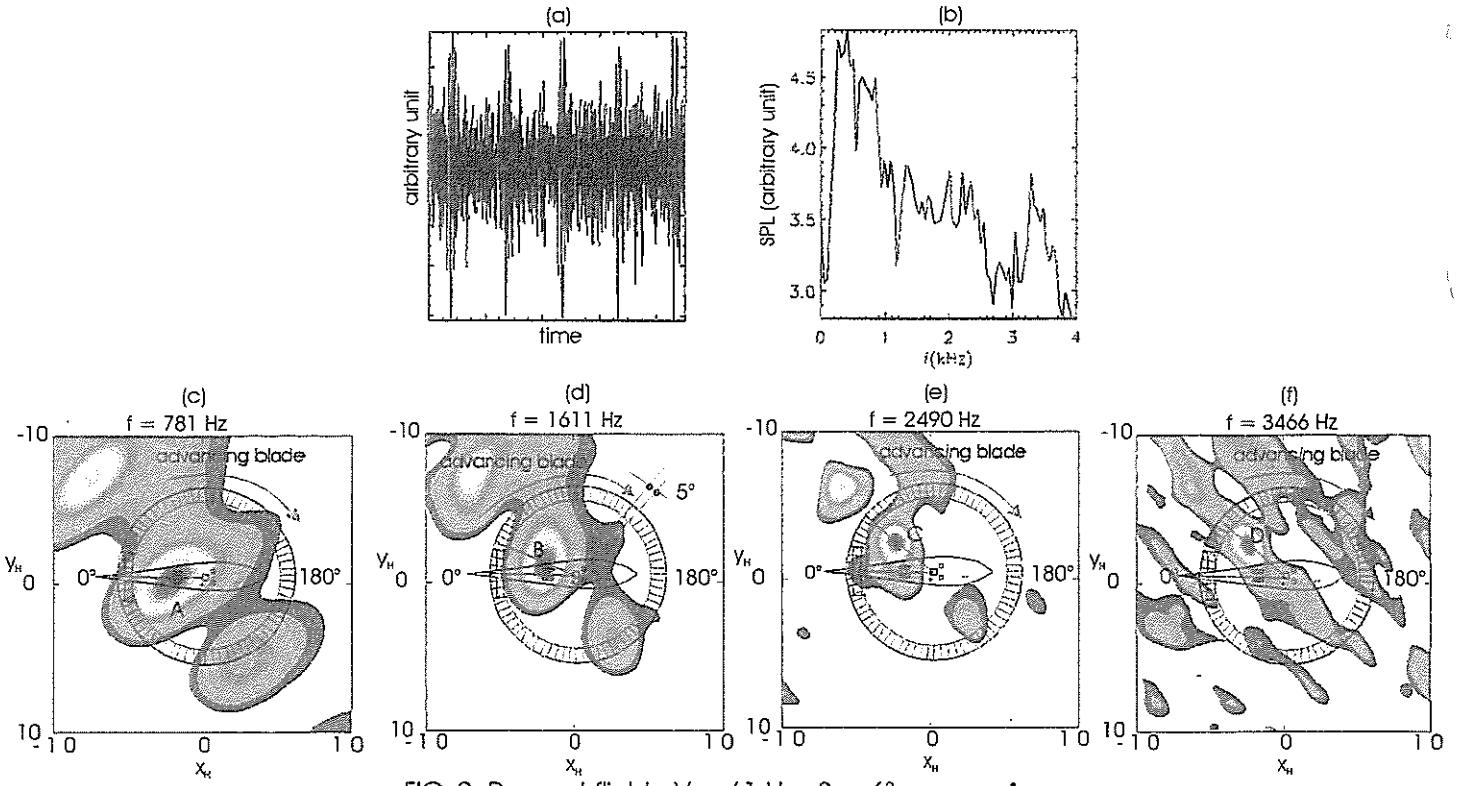

FIG. 9. Descent flight - V = 61 kts - β = 6°.
(a) Acoustic signature of Microphone 8 of the array.
(b) Spectrum of acoustic signature of Microphone 8 of the array.
Localization processing by Method 1 at : (c) 781 Hz; (d) 1611 Hz;
(e) 2490 Hz; (f) 3466 Hz .

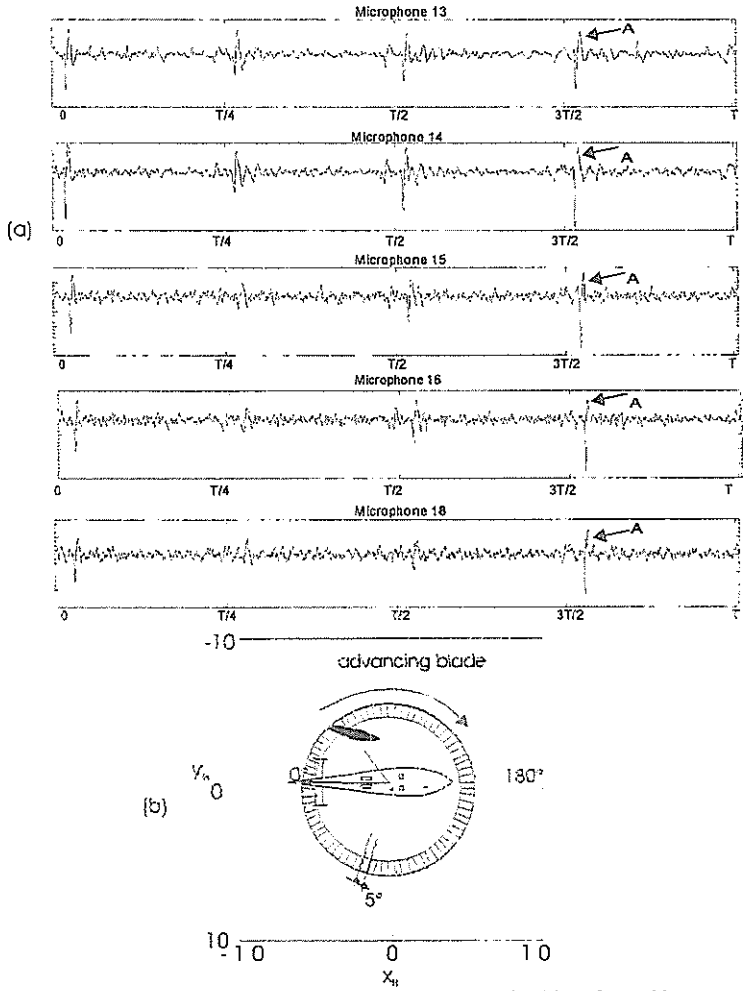

FIG. 10. Descent flight - V = 61 kts - β = 6°;
(a) Acoustic signatures used by Method 2;
(b) Locations of BVI noise A found by Method 2.